RSC Advances

ROYAL SOCIETY OF CHEMISTRY

www.rsc.org/advances

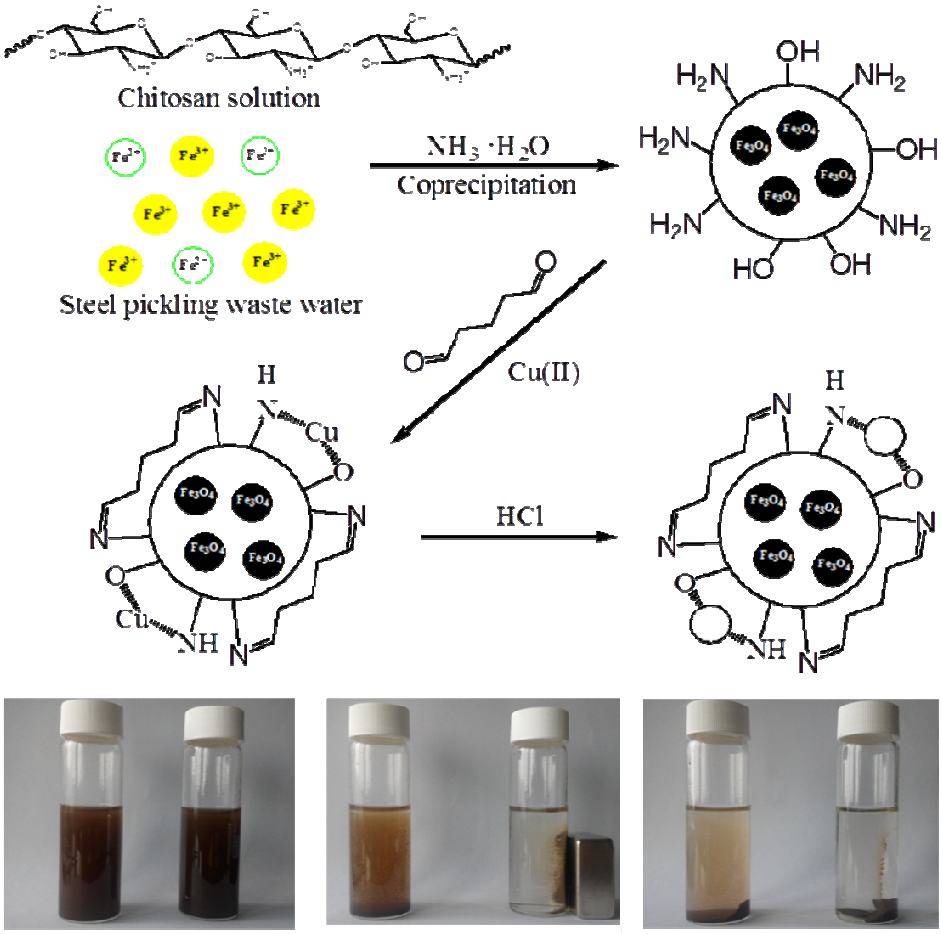

Selective adsorption of Cu(II) from aqueous solution by ion imprinted magnetic chitosan microspheres prepared from steel pickling waste liquor

Yuling Cai[a,b], *Liuchun Zheng*[a,b *], *Zhanqiang Fang*[a,b **]

[a] School of Chemistry and Environment, South China Normal University, Guangzhou, 510006, China;

[b] Guangdong Technology Research Centre for Ecological Management and Remediation of Urban Water System, Guangzhou 510006, China

[*]Corresponding author: Liuchun Zheng

**Corresponding author: Zhanqiang Fang

Correspondence address: School of Chemistry and Environment, South China Normal University, Guangzhou Higher Education Mega Center, Guangzhou 510006, P.R. China

Tel: +86 20 39313279/39310250 Fax: +86 20 39380187 E-mail address: zhqfang@scnu.edu.cn (Zhangqiang Fang); lczhengscnu1@163.com (Liuchun Zheng).

Abstract

In order to reduce cost and improve practicability, an ion imprinted magnetic chitosan (IMCS) was synthesized through co-precipitation using steel pickling waste liquor and chitosan and Cu(II) as template ions, and then was characterized by TEM, SEM, EDX, FTIR, XRD and VSM. The batch experiments were carried out for its potential application and high selectivity of Cu(II) removal due to the paramagnetic property and coordination reactions in the imprinted cavities. Kinetic studies revealed that the adsorption process followed the pseudo second-order model and the equilibrium data fit perfectly with the Langmuir isotherm model while the maximum adsorption capacity was 109.89 mg g^{-1}. Negative values of ΔH^0 and ΔG^0 indicated an exothermic and spontaneous adsorption. The adsorption process was found to be chemical reaction and the coordination complexes were formed between the metal ions and the groups of chitosan binding mainly in the "bridge model". Meanwhile, 0.2 mol L^{-1} HCl solution was considered as the most appropriate eluent for regeneration. It showed a great performance on the experiments of practical copper waste water and the cost was accounted.

Keywords: Magnetic chitosan; Ion imprinted; Copper; Steel pickling waste liquor.

1. Introduction

Large amounts of copper waste water are produced from electroplating industry[1, 2]. To date, numerous technologies have been developed for the Cu(II) removal from the waste water, such as electrodialysis, chemical precipitation, ion exchange, adsorption and membrane filtration[3, 4], while adsorption is one of the most economic, efficient and widely used methods[5]. But lots of absorbents have low selectivity of metal ions and are difficultly separated in aqueous solution, the ion imprinted magnetic adsorbents have been considered increasingly to solve these problems[6, 7].

The ion imprinted polymers have a predetermined selectivity towards the given target ion and are applied widely in solid phase extraction[8]. The cross-linking of linear chain polymers is the maturest technique to prepare ion imprinted polymers, which are mainly used with chitosan, a natural linear polymer[7]. After adsorption, the chitosan-based adsorbents can be very difficult to separate from aqueous solutions by traditional methods and the discharged leftovers may bring secondary pollutions[6]. Magnetic separation can overcome this problem. Chitosan-based adsorbents can be separated under an external magnetic field by combination with magnetic materials[9].

Nowadays, ion imprinted magnetic chitosan materials have been widely used for Cu(II) or other metal ions removal from aqueous solutions. Ren et al.[10] synthesized magnetic Cu(II) ion imprinted chitosan adsorbent for selective removal of copper and the maximum adsorption capacity calculated from the Langmuir isotherm was 71.36 mg g^{-1}. Zhou et al.[11] reported that the ion imprinted magnetic chitosan resins were prepared using U(VI) as template for selectivity adsorption of uranium. And Fan et

al.[12] used a magnetic thiourea-chitosan Ag^+ imprinted absorbent to remove Ag(I) from water environment.

Remarkably, the additional magnetic components of these ion imprinted magnetic chitosan materials were commonly synthesized well using chemical agents before composing with chitosan, which needed expensive chemical agents for iron source and required complicated multi-step synthesis[10-17]. The problems limited their engineering applications.

Our research team has synthesized magnetic absorbent EDA-Fe_3O_4 using steel pickling waste liquor as raw material, which was used to remove Cr(VI) and reduced the treatment cost efficiently[18].

In this study, an ion imprinted magnetic chitosan (IMCS) was produced successfully using the mixture of steel pickling waste liquor and chitosan solution as raw materials and using Cu(II) as the template ion. During the procedure, the magnetic component was synthesized at the same time as the magnetic chitosan composite and dispersed in chitosan. Then the material was characterized and the adsorption process of Cu(II) from aqueous solution was investigated, including the effect of pH, kinetic and isotherm, and the thermodynamic and adsorption mechanism were further studied. The experiments of selectivity and regeneration were also preformed. At last, practical waste water was used in experiments.

2. Materials and methods

2. 1. Chemicals

Steel pickling waste liquor used to prepare Fe_3O_4 and IMCS was obtained from

the Jinlai steel plant in Guangzhou, China, the physical and chemical properties of that could be found in our previous reports[18, 19]. Chitosan (≧95%, deacetylated) was purchased from Aladdin Industrial Corporation (Shanghai, China). Ammonia aqueous (25%~28%), acetic acid (>99%), glutaraldehyde (50%), hydrochloric acid (36%~38%), sodium hydroxide (≧96%) and copper sulfate pentahydrate (≧99%) were analytical grade and were purchased from Guangzhou Chemical Agent Company (Guangzhou, China).

2. 2. Synthesis of adsorbents

The synthesis method of Fe_3O_4 was co-precipitation. First, steel pickling waste liquor was heated in water baths with magnetic stirring and N_2 gas protection, and then ammonia solution was added dropwise until the pH value was around 10.0, Fe_3O_4 particles were obtained after 3 h reaction by heating and stirring.

Chitosan powder (1.0 g) was dissolved in acetic acid and then steel pickling waste liquor (2.5 mL) was added into. The mixture solution was heated in water baths at 80℃ with magnetic stirring and dropping ammonia solution until the pH value around 10.0. After 3 h reactions, the raw magnetic chitosan without cross-linking generated was suspended in $CuSO_4$ solution (100 mg L^{-1}), then glutaraldehyde (5 mL, 5.0%) was added. After that, the template ions Cu(II) were removed from the material using HCl solution (1.0 mg L^{-1}). The process was repeated until no copper ions were detected in the eluent. The material was added into NaOH solution (2.0 mg L^{-1}) and then washed with water. After drying, ion imprinted magnetic chitosan (IMCS) was obtained. Magnetic chitosan (MCS) was prepared in the same steps without

introduction of the template ions.

The synthesis scheme was presented in Fig. 1.

2. 3. Characterization

The surface, morphology and size of IMCS were viewed with transmission electron microscopy (TEM) (Tecnai G20, FEI, USA) and scanning electron microscopy (SEM) (Nova^{TM} NanoSEM 430, FEI, USA). The element composition in the surface of IMCS was determined using energy dispersive X-ray (EDX) by SEM (Nova^{TM} NanoSEM 430, FEI, USA). Fourier transform infrared (FTIR) spectra were used to identify the structure of Fe_3O_4, CS, cross-linking CS, MCS and IMCS using an FTIR spectrophotometer (IRPrestige-21, Shimadzu, Japan). The synthesized particles were characterized by X-ray diffraction (XRD) (D8 Advance, Bruker Corporation, German) using Cu Kα radiation. The magnetic properties of Fe_3O_4 and IMCS were measured by a vibrating sample magnetometer (VSM) (MPMS XL-7, Quantum Design, USA) at temperature 300 K. The particle size distribution of IMCS in water was determined by a laser particle size analyzer (Mastersizer 2000, Malvern, US) using laser diffraction method.

2. 4. Batch experiments

The effect of pH value on the adsorption capacity of IMCS was investigated with 30 mL $CuSO_4$ solution (100 mg L^{-1}) and 0.035 g IMCS in the pH range of 1.0~5.0 for 12 h. For the adsorption kinetics studies, 0.035 g IMCS was suspended in 30 mL $CuSO_4$ solutions of the initial concentration of 90~300 mg L^{-1} at pH 5.0 and 305 K. For the equilibrium adsorption studies, the batch experiments were carried on at Cu(II) concentrations varying from 100 to 350 mg L^{-1} in different temperatures (293~327 K) at pH 5.0 for 8 h. The selectivity experiments were conducted by preparing binary

mixture solutions (Cu(II)/Zn(II), Cu(II)/Ni(II), Cu(II)/Cd(II), Cu(II)/Cr(VI)) with each metal initial concentration being around 300 mg L^{-1}. For desorption and regeneration studies, 0.035 g IMCS was suspended in 30 mL of 300 mg L^{-1} $CuSO_4$ solution (pH 5.0, 308 K). After contact time of 8 h, the adsorbent was collected and washed to remove the un-adsorbed copper ions. Then the adsorbent was agitated with 15.0 mL eluent solution (HCl (0.05~0.2 mol L^{-1}), EDTA (0.05~0.1 mol L^{-1})) for another 8 h, and then the adsorbent was separated and washed with 0.1 mol L^{-1} NaOH and deionized water. After drying and grinding, IMCS was regenerated for adsorption. In practical waste water experiments, adsorption was conducted in batch experiments and 0.2 mol L^{-1} HCl was used as the eluent solution in the desorption process. The concentrations of metal ions were detected by a flame atomic absorption spectrometry (PinAAcle 900T, PerkinElmer, USA). In practical waste water experiments, adsorption was conducted in batch experiments and 0.2 mol L^{-1} HCl was used as the eluent solution in the desorption process. The particle copper waste water was copper plating rinse waste water with preliminary treatment collected from a copper plating plant in Guangzhou, the concentration was 1.15 mg L^{-1} and the initial pH value was 3.11.

Adsorption capacities (Q_e, mg g^{-1}) were calculated as follows:

$$Q_e = \frac{C_0 - C_e}{m} \times V \quad (1)$$

where C_0 (mg L^{-1}) and C_e (mg L^{-1}) are the initial and the equilibrium concentrations of metal ions, respectively. M (g) is the weight of adsorbent whereas V (L) represents the volume of solution.

3. Results and discussion

3.1. Characterization

3. 1. 1. TEM and SEM-EDX

Fig. 2 presents the TEM images of IMCS. As presented in the images, Fe_3O_4 was

below 100 nm and opaque while being covered by chitosan around. The SEM images of IMCS illustrated that the particles of IMCS had diameters ranging from 5 to 50 μm with loose, rough and irregular shaped structure, which was in favor to adsorption. The EDX spectra of the surfaces of IMCS (before and after adsorption) showed that IMCS was mainly composed of the elements of C, N, O and Fe as well as few accounts of S and Cu. The materials were washed after adsorption for removal of some easily releasing copper ions remaining on the surface, and then were characterized for the spectrum as Fig. 2(f). The peaks of copper and sulfur increased obviously after adsorption and the weight ratio of copper was 8.43%, which demonstrated that copper was adsorbed on IMCS and the binding between them might be a stable bond.

3. 1. 2. Particle size distribution in aqueous solution

The particle size distribution in aqueous solution was determined using laser diffraction method. The particle sizes were mainly within 90 μm, 10% of them were within 8.104 μm, 50% within 33.239 μm, 90% within 88.637 μm, a very minor amount of them were beyond 100 μm and the volume-weighted average was 46.690 μm. The particle size of some IMCS particles from laser diffraction method was slightly bigger than that presented in SEM images, possibly because some of those particles aggregated driven by some interactions such as hydrogen bonds or Van der Waals' forces.

3. 1. 3. FT-IR and XRD

The FT-IR spectra of Fe_3O_4, CS, cross-linking CS, MCS, IMCS (before and after

adsorption) are given in Fig. 3(a). The characteristic peaks at 3300~3500 cm^{-1} (C-H and N-H stretch) and 1600~1660 cm^{-1} (C-O and N-H bending) were observed[10]. The bonds at 580 cm^{-1} were indicative to the presence of the Fe-O-Fe bond[20]. Comparing with other materials, the specific adsorption peaks at around 580 cm^{-1} were observed in the spectra of MCS and IMCS, which indicated that Fe_3O_4 was synthesized. The characteristic peak (2880~2920 cm^{-1}) ascribed to C-H stretching of methyl or methylene was found in the spectra of all the chitosan materials[10]. A strong adsorption peak at 1384 cm^{-1} was found in the spectra of MCS and IMCS, which attributed to stretching vibration adsorption of N-H[10]. It was probably because that the structure of the composites was quite different with pure CS and cross-linking CS, there existed more amino groups on the surface so that was easier to form surface imprinting and adsorb metal ions[7]. The spectrum of MCS was the same as that of IMCS, which indicated that ion imprinting would not change the contents of groups of magnetic chitosan. In the spectrum of IMCS after adsorption, a new adsorption peak at 1525 cm^{-1} was found to be the characteristic peak of amide N-H bending vibration (~1560 cm^{-1})[11] and a peak at 617 cm^{-1} appeared was associated with the metal-O stretching vibration[21], which suggested that the coordination was formed between Cu(II) and the functional groups of chitosan ($-NH_2$ and -OH).

The XRD patterns for Fe_3O_4 and IMCS are presented in Fig. 3(b). Eight characteristic peaks for Fe_3O_4 appeared in the pattern, which were consistent with the database (PDF No. 65-3107) and the findings of Zhou et al.[11], and demonstrated that the Fe_3O_4 powder prepared was mainly a cubic structure. Furthermore, six

characteristic peaks for Fe_3O_4 was still observed in the pattern for IMCS. These were also consistent with the finding of Monier et al.[13]. It indicated that Fe_3O_4 generated in the synthesis process of IMCS but was covered by chitosan.

3. 1. 4. Magnetic properties study

The magnetization curves for Fe_3O_4 and IMCS and the separation process from aqueous solution are showed in Fig. 4. The saturation magnetization (M_s) value of Fe_3O_4 powder was 63.33 emu g^{-1} which was close to the pure Fe_3O_4 prepared using chemicals (62.8 emu g^{-1})[22]. M_s of IMCS (22.78 emu g^{-1}) was lower, but it was able to be separated from aqueous solution under an external magnetic field[23], which might be that the magnetic material was covered by non-magnetic material to form shell-core structure, leading to the decrease of the content of magnetic material[24, 25]. Besides, the magnetic moment might be quenched by the electron exchange between the surface atoms of Fe_3O_4 and the ligands of chitosan[26]. Moreover, the IMCS particles would not be aggregated after magnetic separation because of non-hysteresis[22].

3. 2. Effects of pH and contact time on the adsorption and the kinetic studies

Fig. 5 shows the effect of initial pH on adsorption efficiency. When the solution pH was higher than 5.5, precipitation of $Cu(OH)_2$ would be formed[22]. Therefore, the adsorption experiments were carried out at pH below 5.5 in this study. The adsorption efficiency of Cu(II) increased with the increase of the pH value. There were not obviously Cu(II) uptakes at lower pH values and its efficiency was only 8.10% at pH 2.0. When the pH value was higher than 3.0, the adsorption efficiency of Cu(II)

increased significantly and reached the maximum at pH 5.0. These results agreed with Chang's report[27], because the protonation of amino groups of chitosan was produced and a competitive adsorption between H^+ and Cu(II) in the solution occurred at low pH[17]. But at higher pH values, the groups of chitosan became negatively charged and the electrostatic interaction between chitosan and Cu(II) enhanced[28].

The effect of contact time on the adsorption of Cu(II) in different concentrations by IMCS and the pseudo second-order kinetics is given in Fig. 5. The adsorption capacities increased significantly in the first 15 min. At 3 min, the uptakes of Cu(II) reached more than 41 mg g^{-1}; the adsorption capacity was up to 69.66 mg g^{-1} at 15 min in the higher initial concentration (286 mg L^{-1}); After that, the adsorption capacities increased slowly and approached equilibrium after 2 h.

Pseudo first-order and pseudo second-order kinetics were used to test the experimental data, which were given as follows:

$$\ln(Q_{e.cal} - Q_t) = \ln Q_{e.cal} - k_1 t \quad (2)$$

$$\frac{t}{Q_t} = \frac{1}{k_2 Q_{e.cal}^2} + \frac{t}{Q_{e.cal}} \quad (3)$$

where $Q_{e.cal}$ and Q_t were the adsorption capacities (mg g^{-1}) at equilibrium and at time t (min), respectively. k_1 (h^{-1}) and k_2 (g mg^{-1} h^{-1}) were the rate constants of pseudo first-order and pseudo second-order kinetic models, respectively.

The kinetic parameters calculated are listed in Table 1. The correlation coefficient (r^2) values of pseudo second-order kinetic model were greater than 0.99 and the adsorption capacities ($Q_{e.cal}$) calculated from pseudo second-order kinetic model were much closer to the experimental data ($Q_{e.exp}$), but the r^2 values of pseudo

first-order kinetic model were all below 0.90 and it did not match with the experimental data, which indicated that the pseudo second-order kinetic model fit the experimental data much better than pseudo first-order kinetic model and the rate limiting step of the adsorption mechanism for IMCS was chemical adsorption[13].

In order to investigate the rate limiting step in the adsorption process, intraparticle diffusion model was tested as follow:

$$q_t = k_p t^{0.5} + C \quad (4)$$

where k_p was the intraparticle diffusion rate constant (mg g^{-1} $min^{-0.5}$), C was the intercept, the parameters are listed in Table 1.

As shown in Fig. 5(b), there were more than one linear portion observed in the plots, it indicated that the adsorption is affected by two or more steps[17]. As depicted in Table 1, the intraparticle diffusion rate constant in different initial concentrations followed the order: $k_{p,1} > k_{p,2} > k_{p,3}$. The rate limiting steps could be described as follow[17]: (1) surface diffusion stage in which large amount of copper ions from bulk solution were adsorbed rapidly by the exterior surface groups of IMCS, (2) intraparticle diffusion stage in which the copper ions were adsorbed by the interior surface of pores, (3) equilibrium state in which the intraparticle diffusion rate constants were close to zero.

3. 3. *Adsorption isotherm models and the themodynamic parameters*

The adsorption experiments were investigated varying Cu(II) initial concentrations from 100 to 350 mg L^{-1} at different temperature. And the adsorption data was analyzed by four important isotherm models (Eq. S(1) to Eq. S(6)) including

Langmuir, Freundlich, Temkin and Dubinin–Radushkevich (D–R) isotherms with the quality of the fit assessed using the correlation coefficient. The parameters calculated from models are listed in Table 2.

Compared with the other models, the Langmuir model fit better with the experimental data due to the higher correlation coefficients (r^2 > 0.99), which suggested that the process was a monolayer adsorption. The maximum adsorption capacity ($Q_{m.cal}$) calculated from Langmuir model was 109.89 mg g^{-1} which showed a certain advantage comparing with other similar adsorbents (Table 4). Moreover, the adsorption capacity showed a decreasing trend generally as the temperature increased. This trend was in agreement with the studies of many other magnetic chitosan materials[13, 31], which suggested an exothermic reaction. As seen in Table 2, the values of R_L ranged form 0.053 to 0.064, indicating that the adsorption was favorable[29].

The Freundlich constant (n) generally reflected the affinity between adsorbent and adsorbate. As seen in Table 2, the values of n were above 1.0, suggesting that the isotherms were classified as L type isotherms which was indicative of chemical adsorption[30].

Temkin model considering the chemical adsorption fit the experimental data quite well with high correlation coefficients (> 0.96)[30]. In this model, greater A_T value indicated greater affinity between adsorbent and adsorbate[22]. The A_T values increased as the temperature decreased, suggesting that the adsorption was an exothermic reaction.

The correlation coefficients for D-R model were the lowest comparing with the

other models and the model fit worse as the temperature became lower. This suggested that the adsorption was not a physical process and low temperature might promote the chemical adsorption process. In addition, the mean adsorption energy (E) calculated from the constant K was used to estimate the type of adsorption. When the value of E was more than 8 kJ mol^{-1} the adsorption behavior could be predicted as chemical adsorption[32]. In this study, the values of E ranged from 87.71 to 103.14 kJ mol^{-1} and were much greater than 8 kJ mol^{-1}, suggesting a chemical adsorption.

The decrease values of adsorption capacities with elevated temperature indicated the exothermic reaction of adsorption process. The thermodynamic equilibrium constant K_0 was determined by plotting ln(Cs/Ce) versus Cs and extrapolating Cs to zero (Eq. S(7), Eq. S(8))[33]. K_0 decreased with elevated temperature indicating that the adsorption was exothermic[30].

As listed in Table 4, the negative ΔG^0 indicated spontaneous adsorption and the degree of spontaneous of the reaction increased with the decrease of temperature. The negative ΔH^0 indicated that the reaction was exothermic.

3. 4. Adsorption mechanism

Additionally, extensive researches showed that the adsorption of copper ions on chitosan was chemical adsorption due to the coordination complexes between groups of chitosan and copper ions[2, 34, 35].

There were lots of amino and hydyoxyl groups on the surface of IMCS, the lone pair on N atoms and O atoms were supplied to the empty atomic orbital of copper ions, so the coordination complexes formed on the surface of the material[16]. Therefore, the

adsorption on chitosan mainly depended on amino and hydyoxyl groups[35]. Copper ion coordinates in square planar configuration[36].The formations of amino groups chelated with copper ion could be classified as the "bridge model" and the "pendant model"(Fig. 6)[37]. Metal ion was bound with two amino groups in "bridge model", while in "pendant model", metal ion was bound with only one amino group and oxydren atoms could be involved in the coordination[35].

According to the two binding patterns, the maximum adsorption capacity of Cu(II) on IMCS could be calculated thought the following equation[35]:

$$\text{Adsorption capacity (mg g}^{-1}) = \frac{M_{Cu}}{M_{subunit} \times N} \times d \times 1000 \quad (5)$$

where M_{Cu} (63.55 g mol^{-1}) and $M_{subunit}$ (161.18 g mol^{-1}) were the molecule weight of copper and the subunit of chitosan, respectively, N was the the number of subunits needed to form one adsorption site (N = 2 in "bridge model", N = 1 in "pendant model"), d was the share of chitosan in IMCS which was about 0.7. As seen in Figure 6, the calculation based on the "bridge model" was closer to the experimental adsorption capacities, thus the "bridge model" binding pattern would be better suitable to describe the adsorption mechanism in this study.

In addition, raw magnetic chitosan particles were dense inside due to the Fe_3O_4 core so that the template ions were easy to bind on the exterior surface of the material. After cross-linking and template ions removal, the fixed space structure of chitosan chain was formed and most amino groups were fixed for chelation in "bridge model", and the adsorption sites ("imprinted cavities") were concentrated on the exterior surface to make the rapid adsorption in initial time with a short equilibrium time,

which was also consistent with the results of kinetic study.

3. 5. Selectivity adsorption studies

The distribution coefficient (K_d), selectivity coefficient (k) and relative selectivity coefficient (k') could be defined as[10]:

$$K_d = \frac{Q_e}{C_e} \quad (6)$$

$$k = \frac{K_d[Cu(II)]}{K_d[M(II)]} \text{ or } k = \frac{K_d[Cu(II)]}{K_d[Cr(VI)]} \quad (7)$$

$$k' = \frac{k_{imprinted}}{k_{non-imprinted}} \quad (8)$$

where *M(II)* represented the competitive ions Zn(II), Ni(II) and Cd(II). The calculated results are listed in Table 5.

It could be seen that the values of relative selectivity coefficient (k') with different competitive ions were greater than 2.0, suggesting that IMCS had higher adsorption capacity and selectivity of Cu(II) than MCS when existing with other heavy metal ions. And the distribution coefficient (K_d) values of Cu(II) on IMCS were also much greater than those on MCS. The high selectivity properties of IMCS were remarkable mainly oweing to the affinity of the groups for the imprinted ions and the match of charge, size and coordination number of the ions with the generated cavities[38]. But MCS had no the generated cavities.

The effects of different competitive ions on the adsorption of Cu(II) by IMCS and MCS are represented in Table 5. These ions could inhibit the adsorption of Cu(II) on IMCS and MCS, due to the competing adsorption phenomena of different metal ions on the adsorption sites. The effects of different competitive ions followed the

order: Zn(II) > Ni(II) > Cd(II) > Cr(VI). Actually, chitosan already exhibited a great chelating ability to Zn(II)[39] and the adsorption mechanism of Cr(VI) was a negative charged ion in the solution, which was different with the metal cation[14]. Noticeably, the adsorption capacities of Cu(II) on IMCS showed few effects by the existence of different competitive ions but obvious influences on MCS, which indicated that IMCS had generated the imprinted cavities to keep a certain adsorption capacity of Cu(II). The Cu(II) optimized cavities formed with defined geometry, which were sensitive to the size and oxidation state of competing ions[40]. Besides, the adsorption capacity of IMCS was still higher than that on MCS without competitive ions, and Anwei Chen et al. presented the similar results[21]. Therefore, It confirmed that in the ion imprinting process, the template ions were added before cross-linking, which protected the amino groups from cross-linking by chelating metal ions, thus more adsorption sites generated in IMCS.

3. 6. Desorption and reuse

Five adsorption-desorption circles were carried out using different concentration of HCl solution and EDTA solution as eluent (Table 6). The desorption efficiency decreased with the decreasing concentration of eluents. The desorption efficiencies and the adsorption capacities in HCl solution were much higher than those in EDTA solution during the five adsorption-desorption circles. Although EDTA solution was a strong chelating agent, the desorption of Cu(II) on IMCS was not as good as HCl solution. Putting adsorbed IMCS into HCl solution, the amino groups of chitosan protonated[8]. Competing between protonation and chelation, a great amount of

hydrogen from HCl solution replaced the metal ions to occupy the groups and most of the metal ions adsorbed were released[16]. Then the adsorption capacity could regain after washing with NaOH solution to deprotonate. Through synthetical consideration, 0.2 mol L^{-1} HCl solution would be the most appropriate eluent for regeneration.

3. 7. Experiments on practical waste water

As seen in Fig. 7, Cu(II) could not be detected in the treated water in the first three circles and the residual concentration was 0.34 mg L^{-1} at the fourth adsorption which still met the limit of copper in releasing waste water (0.5 mg L^{-1}) based on the emission standard in China.. Table 7 lists the results of Cu(II) one-time removal in copper plating waste water. When the dosage of IMCS was only 0.01 g L^{-1}, the residual concentration of Cu(II) was 0.46 mg L^{-1} after contacting for 4 h, which was very close to the limit but still met the standard.

In order to offer references for development and use of IMCS, the cost of the treatment on the collected copper plating waste water by IMCS was accounting. Since the steel pickling waste liquor was used as iron source to synthesize Fe_3O_4 instead of expensive chemical agents, the cost of IMCS synthesis was much cheaper. It would cost around $0.3 to treat 1 t of the waste water to meet the emission standard.

4. Conclusion

IMCS was successfully synthesized and characterized. The batch experiments showed a great performance to remove Cu(II) from aqueous solution. The process was determined as chemical adsorption. The mechanisms were proposed that the

coordination complexes were formed between the metal ions and the groups of chitosan binding mainly in the “bridge model”. Moreover, IMCS had a higher selectivity of Cu(II) and was less affected by the completing ions than MCS, suggesting that the imprinted cavities played the key role. And Cu(II) from practical waste water could be efficiently removed. Therefore, IMCS has a great developing potential for Cu(II) removal compared with other traditional materials prepared from chemical agent and multi-steps.

Acknowledgements

This research was supported by National Natural Science Foundation of China (No. 41471259) and Guangdong Technology Research Centre for Ecological Management and Remediation of Urban Water Systems (2012gczxA005). The authors are grateful to all study participants and thanks for the financial support of the Guangdong Technology Research Centre for Ecological Management and Remediation of Water Systems.

References

1. C. M. Futalan, C.-C. Kan, M. L. Dalida, C. Pascua and M.-W. Wan, Carbohydr. Polym., 2011, 83, 697-704.
2. F. A. R. Pereira, K. S. Sousa, G. R. S. Cavalcanti, M. G. Fonseca, A. G. de Souza and A. P. M. Alves, Int. J. Biol. Macromol, 2013, 64, 471-478.
3. F. Fu and Q. Wang, J. Environ. Manage., 2011, 92, 407-418.
4. M. Hua, S. Zhang, B. Pan, W. Zhang, L. Lv and Q. Zhang, J. Hazard. Mater., 2012, 211-212, 317-331.
5. P. D. Chethan and B. Vishalakshi, Carbohyd. Polym., 2013, 97, 530-536.
6. D. H. Reddy and S. M. Lee, Adv. Colloid Interfac., 2013, 201-202, 68-93.
7. C. Branger, W. Meouche and A. Margaillan, React. Funct. Polym., 2013, 73, 859-875.
8. X. Luo, Y. Huang, F. Deng, S. Luo, Y. Zhan, H. Shu and X. Tu, Microchim. Acta., 2012, 179, 283-289.
9. G. Dodi, D. Hritcu, G. Lisa and M. I. Popa, Chem. Eng. J., 2012, 203, 130-141.
10. Y. Ren, M. Zhang and D. Zhao, Desalination, 2008, 228, 135-149.
11. L. Zhou, C. Shang, Z. Liu, G. Huang and A. A. Adesina, J. Colloid. Interface. Sci., 2012, 633, 165-172.
12. L. Fan, C. Luo, Z. Lv, F. Lu and H. Qiu, J. Hazard. Mater., 2011, 194, 193-201.
13. M. Monier, D. M. Ayad, Y. Wei and A. A. Sarhan, J. Hazard. Mater., 2010, 177, 962-970.
14. X. Hu, J. Wang, Y. Liu, X. Li, G. Zeng, Z. Bao, X. Zeng, A. Chen and F. Long, J. Hazard. Mater., 2011, 185, 306-314.
15. M. Monier and D. A. Abdel-Latif, J. Hazard. Mater., 2012, 209-210, 240-249.
16. S. P. Kuang, Z. Z. Wang, J. Liu and Z. C. Wu, J. Hazard. Mater., 2013, 260, 210-219.
17. Y. Ren, H. A. Abbood, F. He, H. Peng and K. Huang, Chem. Eng. J., 2013, 226, 300-311.
18. X. B. Fang, Z. Q. Fang, P. K. E. Tsang, W. Cheng, X. M. Yan and L. C. Zheng, Appl. Surf. Sci., 2014, 314, 655-662.
19. Z. Fang, X. Qiu, J. Chen and X. Qiu, Appl. Catal. B: Environ., 2010, 100, 221-228.
20. C. Yuwei and W. Jianlong, Chem. Eng. J., 2011, 168, 286-292.
21. A. Chen, G. Zeng, G. Chen, X. Hu, M. Yan, S. Guan, C. Shang, L. Lu, Z. Zou and G. Xie, Chem. Eng. J., 2012, 191, 85-94.
22. H. Yan, L. Yang, Z. Yang, H. Yang, A. Li and R. Cheng, J. Hazard. Mater., 2012, 229-230, 371-380.
23. Z. Y. Ma, Y. P. Guan and H. Z. Liu, J. Polym. Sci., Part A: Polym. Chem., 2005, 43, 3433-3439.
24. Z. Liu, H. Bai and D. D. Sun, New J. Chem., 2011, 35, 137-140.
25. B. Feng, R. Y. Hong, Y. J. Wu, G. H. Liu, L. H. Zhong, Y. Zheng, J. M. Ding and D. G. Wei, J. Alloys Compd., 2009, 473, 356-362.

26. D. A. van Leeuwen, J. M. van Ruitenbeek, L. J. de Jongh, A. Ceriotti, G. Pacchioni, O. D. Haberlen and N. Rosch, Phys. Rev. Lett., 1994, 73, 1432-1435.
27. Y. C. Chang and D. H. Chen, J. Colloid Interf. Sci., 2005, 283, 446-451.
28. D. Jie, Y. Han, Y. Hu and C. Rongshi, Chem. Eng. J., 2010, 165, 240-249.
29. K. R. Hall, L. C. Eagleton, A. Acrivos and T. Vermeulen, Ind. Eng. Chem. Fund., 1966, 5, 212-223.
30. H. K. Boparai, M. Joseph and D. M. O'Carroll, J. Hazard. Mater., 2011, 186, 458-465.
31. S. Zhang, Y. Zhou, W. Nie, L. Song and T. Zhang, Ind. Eng. Chem. Res., 2012, 51, 14099-14106.
32. Y. Liu, M. Chen and H. Yongmei, Chem. Eng. J., 2013, 218, 46-54.
33. R. Calvet, Environ. Health. Persp., 1989, 83, 145.
34. J. R. Rangel-Mendez, R. Monroy-Zepeda, E. Leyva-Ramos, P. E. Diaz-Flores and K. Shirai, J. Hazard. Mater., 2009, 162, 503-511.
35. K. Yu, J. Ho, E. McCandlish, B. Buckley, R. Patel, Z. Li and N. C. Shapley, Colloid. Surface. A., 2013, 425, 31-41.
36. S. Z. Bajwa and P. A. Lieberzeit, Sens. Actuators B., 2015, 207, 976-980.
37. O. A. C. Monteiro and C. Airoldi, J. Colloid Interf. Sci., 1999, 212, 212-219.
38. S. C. Pinheiro, A. B. Descalzo, I. M. Raimundo, Jr., G. Orellana and M. C. Moreno-Bondi, Anal. Bioanal. Chem., 2012, 402, 3253-3260.
39. C.-Y. Chen, C.-Y. Yang and A.-H. Chen, J. Environ. Manage., 2011, 92, 796-802.
40. S. Z. Bajwa, R. S. Z. Bajwa and P. A. Lieberzeit, Sens. Actuators B., 2014, 192, 522-528.
41. M. Monier, D. M. Ayad and D. A. Abdel-Latif, Colloids Surf., B, 2012, 94, 250-258.
42. H. L. Vasconcelos, T. P. Camargo, N. S. Gonçalves, A. Neves, M. Laranjeira and V. T. Fávere, React. Funct. Polym., 2008, 68, 572-579.

Figures

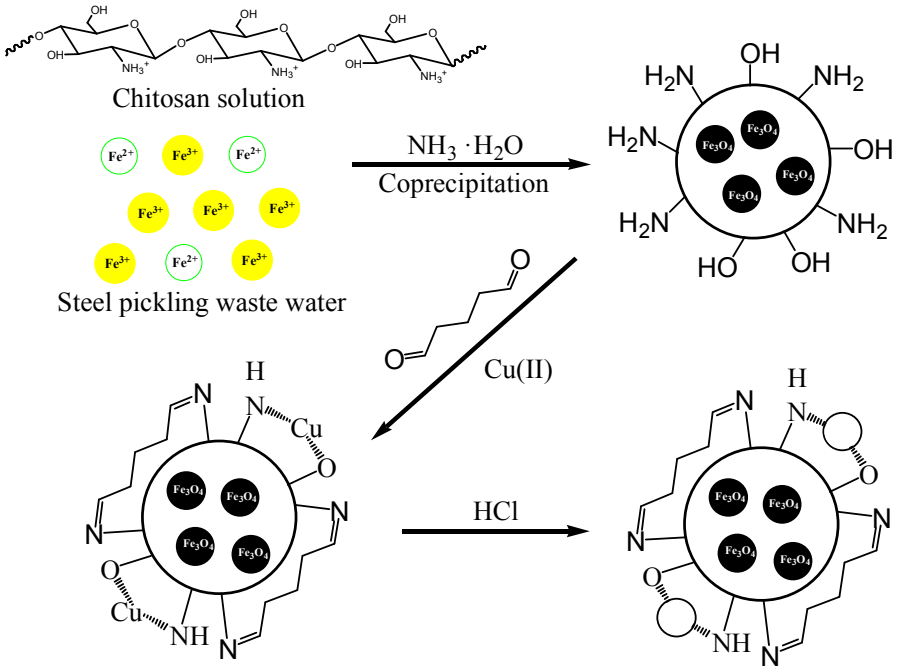

Fig. 1. Synthetic strategy for IMCS

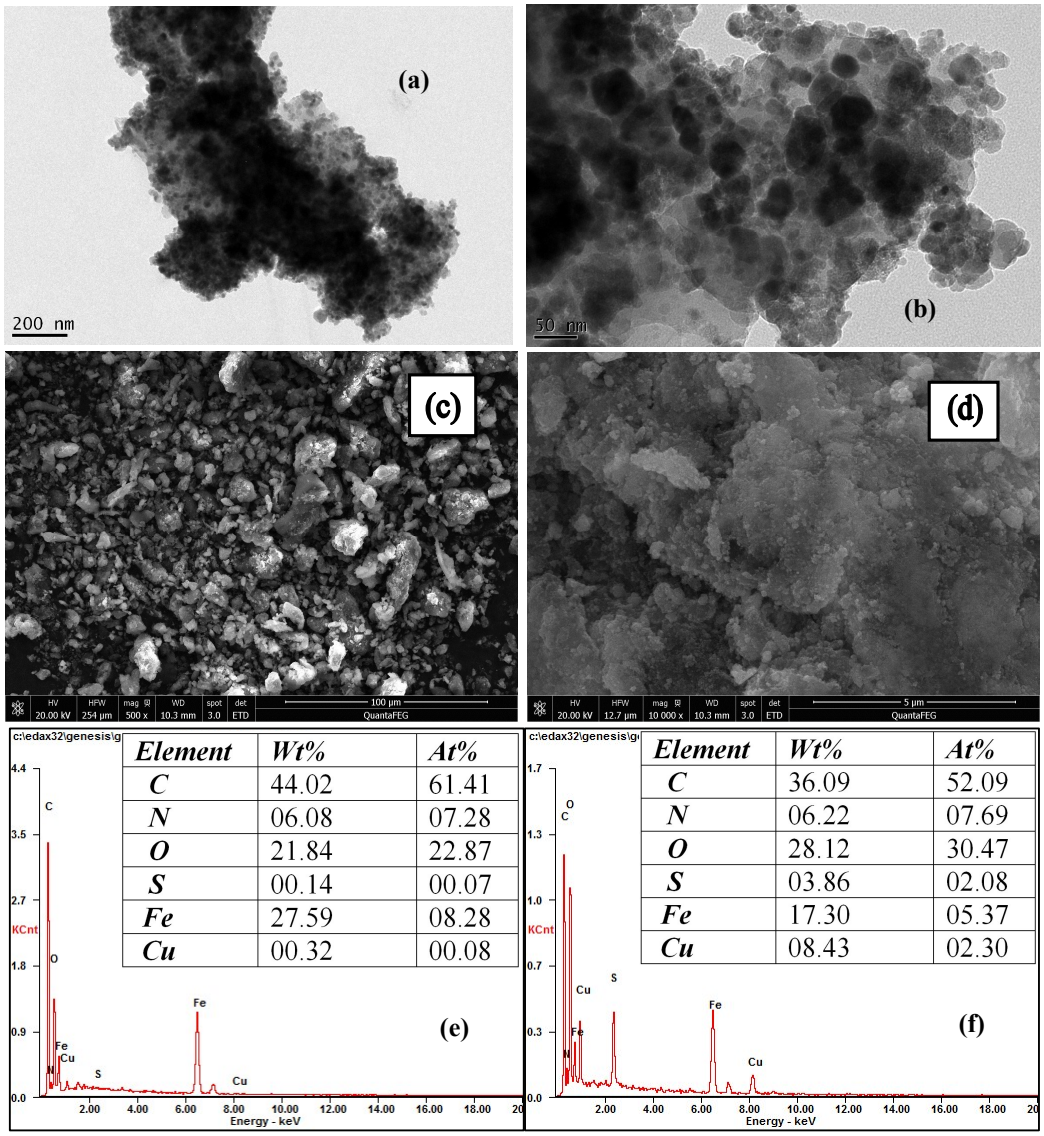

Fig. 2. TEM images of IMCS under different magnifications: (a) 160 000, (b) 500 000, and SEM-EDX micrographs of IMCS: SEM images of IMCS before adsorption at magnification of 500 (c), 10 000 (d) and EDX spectrum of IMCS before (e) and after (f) adsorption .

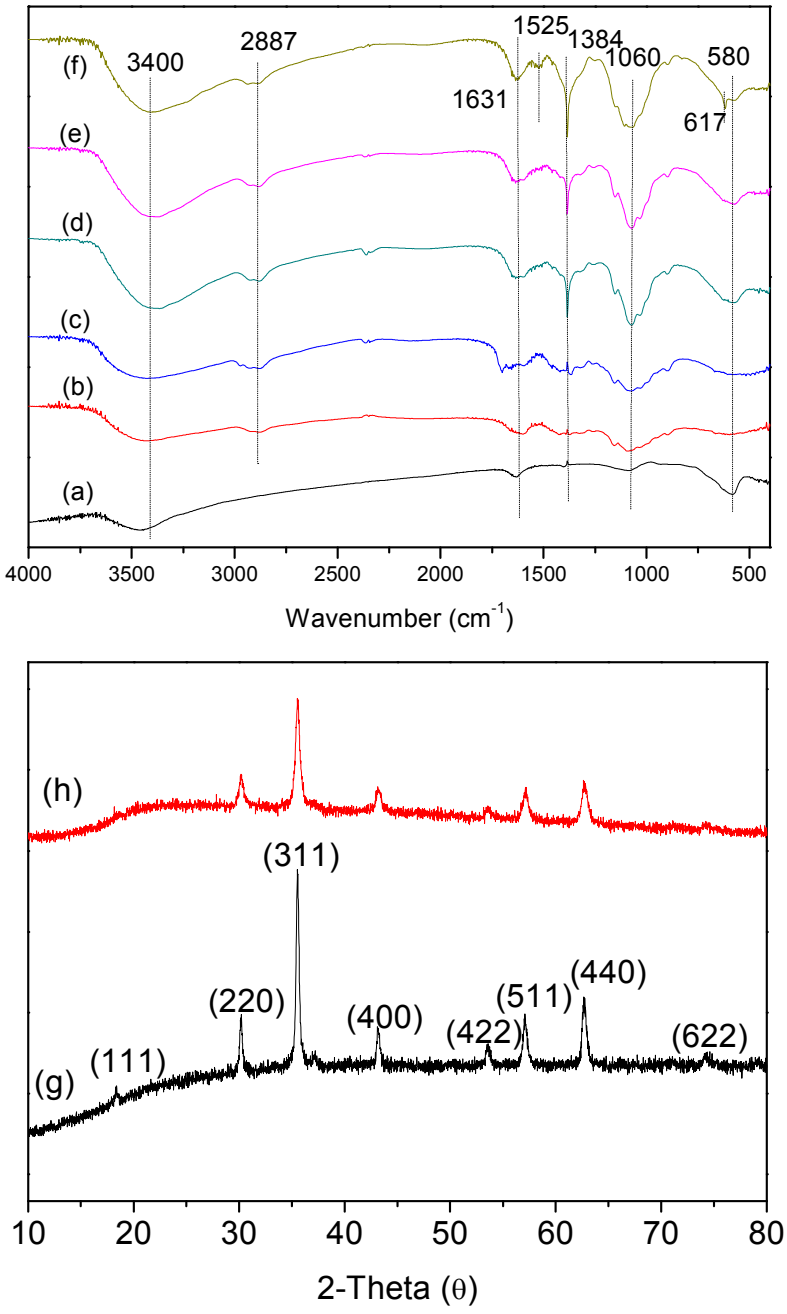

Fig. 3. FTIR spectra of Fe_3O_4 (a), CS (b), cross-linking CS (c), MCS (d), IMCS (before (e) and after (f) adsorption) and XRD patterns for Fe_3O_4 (g) and IMCS (h).

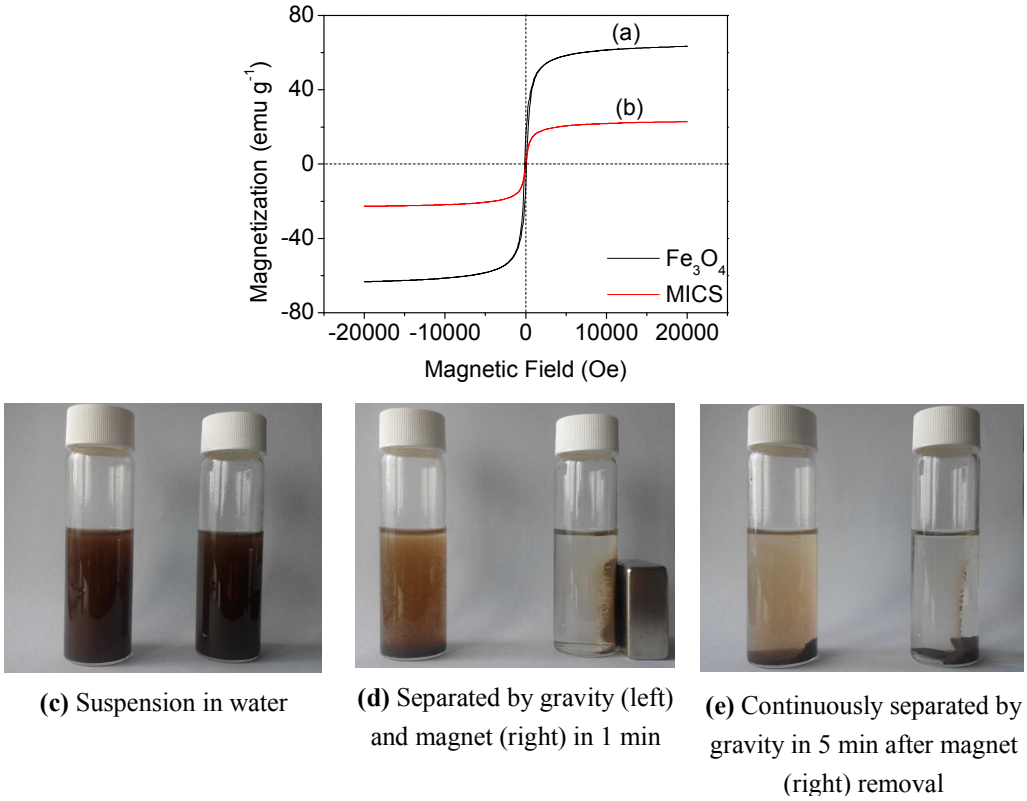

(c) Suspension in water

(d) Separated by gravity (left) and magnet (right) in 1 min

(e) Continuously separated by gravity in 5 min after magnet (right) removal

Fig. 4. Magnetization curves of Fe_3O_4 nanoparticle (a) and IMCS (b) at 300 K and the separation process of IMCS.

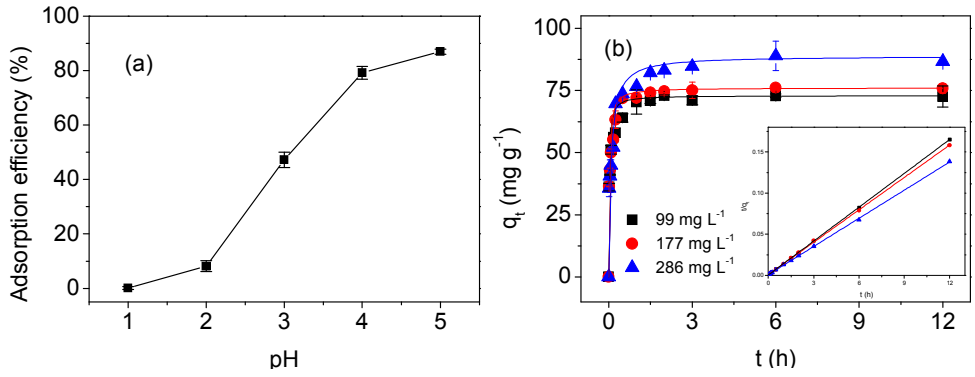

Fig. 5. Effect of initial pH (a) (Dosage: 1.17 g L^{-1}; Temperature: 303 K; Initial concentration: 100 mg L^{-1}; Adsorption time: 12 h.) and contact time (b) and pseudo second-order kinetics (inset) of Cu(II) adsorption onto IMCS. (pH = 5.0; Temperature: 303 K; Dose: 0.035 g 30 mL^{-1}; Initial concentration: 90~300 mg L^{-1}.)

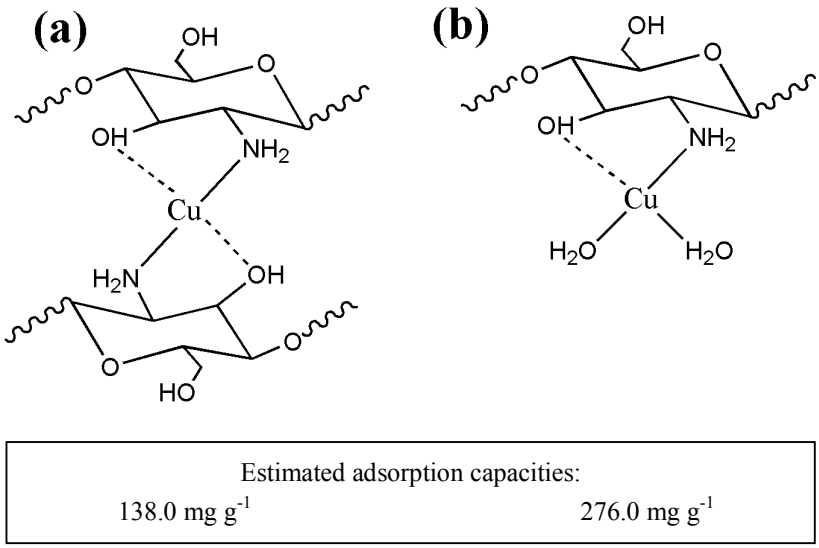

Fig. 6. Formation of chitosan chelates with copper ion (a) bridge model (b) pendant model[36].

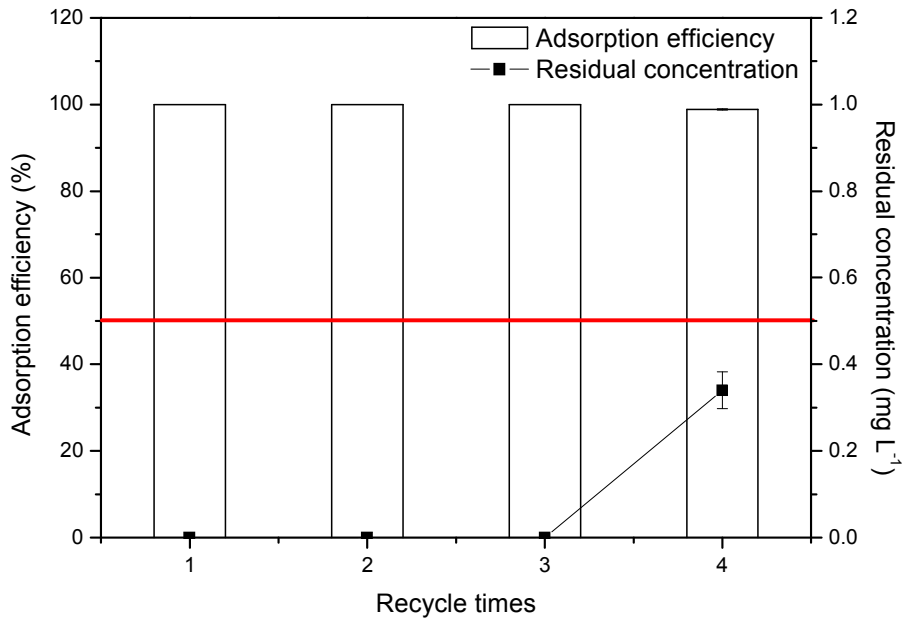

Fig. 7. Removal efficiency and residual concentration of Cu(II) in medium Cu(II) concentration copper plating rinse waste water. (Initial dosage: 0.1 g L^{-1}; pH=5.0; Temperature: 308 K; Cu(II) concentration of sample water: 1.15 mg L^{-1}; Adsorption time: 4 h; Desorption time: 8 h; Eluent: 0.2 mol L^{-1} HCl.)

Tables

Table 1 Adsorption kinetic model rate constants and Intraparticle diffusion model parameters for Cu(II) adsorption on IMCS

C_0 (mg L^{-1})	$Q_{e.exp}$ (mg g^{-1})	Pseudo first order			Pseudo second order			Intraparticle diffusion model								
		k_1 (h^{-1})	$Q_{e.cal}$ (mg g^{-1})	r^2	$k_2\times10^{-7}$ (g mg^{-1} h^{-1})	$Q_{e.cal}$ (mg g^{-1})	r^2	$k_{p,1}$	$k_{p,2}$	$k_{p,3}$ (mg g^{-1} $min^{-0.5}$)	C_1	C_2	C_3	r_1^2	r_2^2	r_3^2
99	72.97	0.34	14.71	0.73	1.03	72.99	>0.99	62.20	24.68	-0.19	29.24	45.98	73.25	0.92	0.99	0.96
177	75.97	0.42	12.41	0.79	1.03	76.34	>0.99	70.56	15.41	0.52	27.75	55.84	74.06	0.97	0.81	0.95
286	87.28	1.01	35.25	0.89	1.17	87.72	>0.99	59.48	15.10	3.61	27.71	62.39	78.17	0.99	0.97	0.90

Table 2 Langmuir, Freundlich, Temkin, D-R isotherm model parameters and correlation coefficients for adsorption at different temperatures

Temperature	Langmuir				Freundlich			Temkin			D-R			
(K)	$Q_{m.cal}$ (mg g^{-1})	K_L (L mg^{-1})	R_L[a]	r^2	K_F (mg g^{-1})	n	r^2	A_T (mg g^{-1})	B_T (mg g^{-1})	r^2	Q_{DR} (mg g^{-1})	$K\times10^{-5}$	E (kJ mol^{-1})	r^2
293	108.70	0.051	0.053	0.9976	93.99	5.47	0.9511	3.29	15.19	0.9629	93.49	-4.7	103.14	0.8563
298	109.89	0.046	0.058	0.9972	73.05	4.98	0.9481	2.00	16.50	0.9612	93.70	-5.5	95.35	0.8691
309	109.89	0.043	0.063	0.9997	58.44	4.65	0.9854	1.39	14.50	0.9922	92.67	-5.6	94.49	0.8667
317	108.70	0.042	0.063	0.9987	54.96	4.62	0.9695	1.34	17.41	0.9816	92.48	-5.9	92.06	0.8995
327	105.26	0.042	0.064	0.9983	46.42	4.50	0.9615	1.17	17.32	0.9647	90.70	-6.5	87.71	0.9186

[a]$C_0 \approx 350$ mg L^{-1}.

Table 3 Comparison of maximum adsorption capacities of various adsorbents for Cu(II) obtained by Langmuir model.

Adsorbents	pH	Temperature (K)	[a]$C_{e.max}$ (mg L^{-1})	$Q_{m.cal}$ (mg g^{-1})	Reference
Monodisperse chitosan-bound Fe_3O_4 nanoparticles	5.0	300	> 1600	21.5	27
CS-MCM	5.5	303	> 300	108.0	22
CS/PAA-MCM	5.5	303	> 350	174.0	22
Magnetic chitosan nanoparticles	5.0	308.15	> 200	35.5	20
Cross-linked magnetic chitosan-2-aminopyridine glyoxal Schiff's base	5.0	303	> 275	124	41
Chitosan crosslinked with a metal complexing agent	6.0	300	> 180	113.6	42
Cross-linked magnetic chitosan-isatin Schiff's base resin	5.0	301	> 250	103.16	13
EDTA functionalized magnetic nano-particles	6.0	298	< 6	46.27	32
Novel magnetic ion-imprinted chitosan	5.0	298	219.74	109.86	This study

[a]$C_{e.max}$ means the maximum of the equilibrium concentrations.

Table 4 thermodynamic parameters for adsorption at different temperatures

Temperature (K)	K_0	ΔG^0 (kJ mol^{-1})	ΔH^0 (kJ mol^{-1})	ΔS^0 (J mol^{-1} K^{-1})	r^2
293	80.83	-10.70			
298	49.08	-9.65			
309	39.61	-9.45	-21.59	38.65	0.89
317	35.75	-9.43			
327	28.17	-9.08			

Table 5 The selectivity parameters of IMCS and MCS for Cu(II)

Metal ions	Adsorbent	Q_e(Cu) (mg g^{-1})	K_d(Cu)	K_d(X)	k	k'
Cu(II)	MCS	100.28	-	-	-	-
	IMCS	95.07	-	-	-	
Cu(II)/Zn(II)	MCS	79.16	0.062	0.023	2.693	14.430
	IMCS	55.76	0.096	0.002	38.866	
Cu(II)/Ni(II)	MCS	82.89	0.083	0.046	1.795	3.956
	IMCS	69.04	0.108	0.015	7.103	
Cu(II)/Cd(II)	MCS	84.00	0.076	0.025	2.989	10.600
	IMCS	64.71	0.104	0.003	31.679	
Cu(II)/Cr(VI)	MCS	84.43	0.075	0.071	1.067	2.154
	IMCS	85.97	0.105	0.046	2.297	

Table 6 Desorption and regeneration performance of IMCS in different eluents

Recycle time	0.2 mol L^{-1} HCl		0.1 mol L^{-1} HCl		0.05 mol L^{-1} HCl		0.1 mol L^{-1} EDTA		0.05 mol L^{-1} EDTA	
	Adsorption capacity (mg g^{-1})	Desorption efficiency (%)	Adsorption capacity (mg g^{-1})	Desorption efficiency (%)	Adsorption capacity (mg g^{-1})	Desorption efficiency (%)	Adsorption capacity (mg g^{-1})	Desorption efficiency (%)	Adsorption capacity (mg g^{-1})	Desorption efficiency (%)
1	98.63	100.87	99.08	98.58	98.84	95.58	98.79	94.59	99.55	93.60
2	96.52	98.01	92.73	93.93	89.08	93.47	87.06	91.88	84.57	88.47
3	96.57	97.51	94.65	94.18	88.26	91.24	83.83	82.57	81.83	80.60
4	95.98	93.46	94.30	91.21	83.74	89.13	80.97	81.67	72.80	80.79
5	93.82	91.77	91.68	88.50	76.22	87.70	69.50	79.89	68.05	74.35

Table 7 Results for copper ion one-time removal in copper plating rinse waste water (Sample volume: 200 mL, shaking time: 4 h, temperature: 308 K)

Sample water	pH	Copper found (mg L^{-1})	Adsorbent dosage (g L^{-1})	Equilibrium concentration (mg L^{-1})	Removal efficiency
Copper plating rinse waste water	5.0	1.15	0.01	0.46	98.44%